

Tuning of a Class of Reset Elements Using Pseudo-Sensitivities*

Ali Ahmadi Dastjerdi¹, Niranjana Saikumar¹ and S.H. HosseinNia¹

Abstract—Currently, the demand for a better alternative to linear PID controllers is increasing due to the rising expectations of the high-tech industry. In literature, it has been shown that Constant in gain Lead in phase (CgLp) compensators, which are a type of reset element, have high potential to improve the performance of systems. Although there are few works which investigate tuning of these compensators, the high order harmonics and steady-state performances have not yet been considered in these methods. Recently, a frequency-domain framework has been developed to analyze closed-loop performances of reset control systems which includes high order harmonics. In this paper, this frequency-domain framework is combined with loop-shaping constraints to provide a reliable frequency-domain tuning method for CgLp compensators. Finally, different performance metrics of a CgLp compensator are compared with those of a PID controller on a precision positioning stage. The results show that the presented tuning method is effective, and the system with the CgLp compensator achieves superior dynamic performance to that of the PID controller.

I. INTRODUCTION

The fast rising high-tech industry leads researchers to find a better alternative for linear controllers [1]. One of the appropriate alternatives is reset element which has gained a lot of attention due to its simple configuration [2]–[7]. In 1958, the first reset element was introduced by Clegg [4]. Clegg Integrator (CI) is an integrator which resets its state to zero when its input crosses zero. Then, First Order Reset Element (FORE) [2], [8] and Second Order Reset Element (SORE) [6], [8] have been developed to provide more design freedom and applicability. Other reset conditions such as reset band [9], [10] and fixed reset instants [11] have also been studied. In order to soften non-linearities of reset elements, several techniques like partial reset and PI+CI approaches have been proposed [12].

Based on Describing Function (DF) analysis, it can be seen that reset controllers provide less lag phase in comparison with their base linear structures. This phase advantage is utilized to introduce new compensators [8], [13], [14]. One of these reset compensators is 'Constant in gain Lead in phase' (CgLp) whose gain is constant while providing a phase lead [8], [15]. In these works, CgLp has been used as an alternative for the derivative to compensate part of the required phase lead. This is advantageous because the open-loop will have higher gains at low frequencies and lower

gains at high frequencies which results in higher precision performances.

There are few studies which investigate tuning of CgLp compensators [8], [15], [16]. In those works, CgLp is tuned to get a specific amount of phase lead at the cross-over frequency. However, as a result of the design flexibility of reset controllers, various combinations of tuning parameters could be used to provide the same open-loop phase compensation at the cross-over frequency based on the DF analysis. However, not all sets of tuning parameters result in performance improvement. In addition, stability has not been assessed in tuning method and has to be checked with non-linear stability methods, separately. Furthermore, the existence of the steady-state performance of the closed-loop has not been assured in those works. Thus, there is a lack of reliable tuning method for CgLp compensators.

Recently, a new frequency-domain framework is developed which analyzes the closed-loop steady-state performances of reset control systems considering high order harmonics [17]. Moreover, a frequency-domain method for assessing the stability of reset elements has been proposed [18]. In this paper, we combined the frequency-domain framework [17], the frequency-domain stability method [18], the DF method, and loop-shaping constraints to provide a reliable tuning method for CgLp compensators. Finally, to show the effectiveness of the proposed tuning method, a CgLp compensator is tuned and implemented on a precision positioning stage.

In the remainder of this paper, the tuning method is elaborated in Section II. In Section III, a tuned CgLp compensator is applied to a precision positioning stage, and its performance is compared with a PID controller. Conclusions and remarks for further study are provided in Section IV.

II. TUNING METHOD

In this section, first, frequency-domain descriptions for reset elements, CgLp compensators, the stability condition, and pseudo-sensitivities (sensitivity functions defined for nonlinear controllers) are briefly recalled. Then the structure of the controller is introduced, and the tuning method is proposed.

A. Frequency Analysis of Reset Elements

The state-space representation of reset elements is

$$\begin{cases} \dot{x}_r(t) = A_r x_r(t) + B_r e(t), & e(t) \neq 0, \\ x_r(t^+) = A_\rho x(t), & e(t) = 0, \\ u(t) = C_r x(t) + D_r e(t), \end{cases} \quad (1)$$

*This work was supported by NWO, through OTP TTW project #16335.

¹A. Ahmadi Dastjerdi, N.saikumar and S.H. HosseinNia are with the Faculty of Department of Precision and Microsystems Engineering, Delft University of Technology, Delft, The Netherlands. A.AhmadiDastjerdi@tudelft.nl, N.saikumar@tudelft.nl, and s.h.hosseinniakani@tudelft.nl

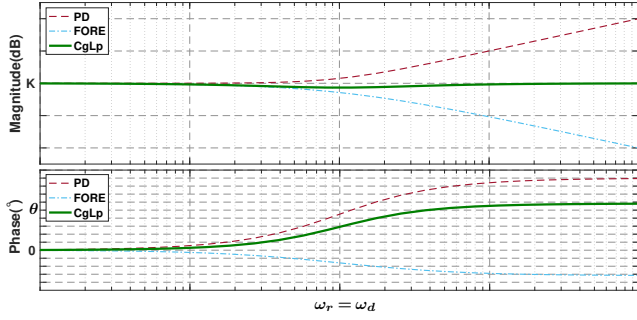


Fig. 1: The DF of a CgLp compensator

in which A_r , B_r , C_r and D_r are the state matrices of the base linear system, $e(t)$ and $u(t)$ are the error input and control input, respectively. The resetting matrix A_ρ determines states' values after reset action. Since reset elements are non-linear, the DF analysis is popularly used in literature to study their frequency behaviour. To have a well-defined steady-state response, it is required that A_r has all eigenvalues with negative real part and $A_\rho e^{\frac{A_r \pi}{\omega}}$ has all eigenvalues with magnitude smaller than one [3]. The sinusoidal input DF of reset elements (1) is given in [3] as

$$\mathcal{N}(j\omega) = C_r(j\omega I - A_r)^{-1} B_r(I + j\Theta(\omega)) + D_r, \quad (2)$$

where Θ is

$$\Theta(\omega) = \frac{-2\omega^2}{\pi} (I + e^{\frac{\pi A_r}{\omega}}) \left((I + A_\rho e^{\frac{\pi A_r}{\omega}})^{-1} A_\rho (I + e^{\frac{\pi A_r}{\omega}}) - I \right) (\omega^2 I + A_r^2)^{-1}. \quad (3)$$

B. CgLp Compensator

A CgLp compensator (4) is constructed using a FORE or a SORE with the series combination of a corresponding order of a lead filter. Considering the DF analysis, this compensator has a constant gain with a lead phase (Fig. 1) ([8], [19]). In this paper, we only consider the first order CgLp which is

$$C_{CgLp}(s) = \left(\frac{1}{\frac{s}{\omega_r} + 1} \right) \left(\frac{\frac{s}{\omega_d} + 1}{\frac{s}{\omega_r} + 1} \right), \quad (4)$$

where ω_r is the corner frequency of the reset element, $A_\rho = \gamma$ is the reset matrix, and ω_d and ω_f are the corner frequencies of the lead filter. To have a constant gain, corner frequencies ω_d and ω_r are almost equal (there is a small correction factor which is provided in [8]) and $\omega_f \gg \omega_r$.

C. H_β Condition

There are several theories to determine the stability of reset control systems [5], [7], [12], [20]. Among those, the H_β condition presented in [5], [7], [18] gets a lot of attention. In [18], a method is developed to examine the H_β conditions utilizing the frequency response of the plant. To this end, consider $L(j\omega)$ and $C_R(j\omega)$ as the base linear frequency

responses of the open-loop and of the reset element, respectively. Then, the Nyquist Stability Vector (NSV= $\vec{\mathcal{N}}(\omega) \in \mathbb{R}^2$), for all $\omega \in \mathbb{R}^+$, is $\vec{\mathcal{N}}(\omega) = [\mathcal{N}_\chi \quad \mathcal{N}_\Upsilon]^T$ in which

$$\mathcal{N}_\chi = \left| L(j\omega) + \frac{1}{2} \right|^2 - \frac{1}{4},$$

$$\mathcal{N}_\Upsilon = \Re(L(j\omega) \cdot C_R(j\omega)) + \Re(C_R(j\omega)).$$

Theorem 1: Considering $\theta_1 = \min_{\omega \in \mathbb{R}^+} \angle \vec{\mathcal{N}}(\omega)$ and $\theta_2 = \max_{\omega \in \mathbb{R}^+} \angle \vec{\mathcal{N}}(\omega)$. Suppose $-1 < \gamma \leq 1$, then, the H_β condition for a reset control system is satisfied and its response is uniformly bounded-input bounded-state (UBIBS) for any bounded input if [18]

$$\left(-\frac{\pi}{2} < \theta_1 < \pi \right) \wedge \left(-\frac{\pi}{2} < \theta_2 < \pi \right) \wedge (\theta_2 - \theta_1 < \pi). \quad (5)$$

D. Pseudo-Sensitivities for Reset Control Systems

In linear systems, the relation between reference signal $r(t)$ to error $e(t)$ can be calculated by sensitivity transfer functions [21]. Although it is possible to use the DF of the reset elements in those sensitivity transfer functions to analyze the tracking performance of CgLp compensators, it is not a reliable approach because high order harmonics are neglected. In order to analyze reset control systems more accurately, a pseudo-sensitivity function $S_\infty(j\omega)$ for a sinusoidal reference $r = r_0 \sin(\omega t)$ is defined in [17].

Theorem 2: A closed-loop reset control system has a well-defined steady-state solution for any Bohl function input if the H_β condition is satisfied and reset instants have the well-posedness property [17].

In addition, if Theorem 2 holds, the tracking error of the reset control system is a periodic function with the period $\frac{2\pi}{\omega}$. Thus, the pseudo-sensitivity for a reset control system is defined as the ratio of the maximum tracking error of the system to the magnitude of the reference at each frequency.

Definition 1: Pseudo-sensitivity S_∞

$$\forall \omega \in \mathbb{R}^+ : S_\infty(j\omega) = e_{\max}(\omega) e^{j\varphi_{\max}},$$

where

$$e_{\max}(\omega) = \left(\frac{\max_{t_{ss0} \leq t \leq t_{ssm}} (r(t) - y(t))}{|r|} \right) = \sin(\omega t_{\max}) - \frac{y(t_{\max})}{r_0},$$

$\varphi_{\max} = \frac{\pi}{2} - \omega t_{\max}$, $y(t)$ is the response of the closed-loop reset control system, and t_{ss0} and $t_{ssm} = t_{ss0} + \frac{2\pi}{\omega}$ are the steady-state reset instants of the closed-loop reset control system ($e(t_{ss0}) = e(t_{ssm}) = 0$). In a similar way, the pseudo-control sensitivity $CS_\infty(\omega)$, the pseudo-complementary sensitivity $T_\infty(\omega)$, and the pseudo-process sensitivity $PS_\infty(\omega)$ are defined in [17]. These calculations are embedded in a user-friendly toolbox [22].

E. Problem Formulation

In this section, the tuning procedure is explained. For this purpose, a CgLp compensator along with a PID controller is

considered for tuning as

$$C_{CgLP}(s) = K_p \underbrace{\left(\frac{1}{\frac{\alpha s}{\omega_r} + 1} \right)}_{CgLP} \underbrace{\left(\frac{s}{\omega_r} + 1 \right) \left(\frac{s}{\omega_f} + 1 \right)}_{PID} \underbrace{\left(1 + \frac{\omega_i}{s} \right)}_{PI} \underbrace{\left(\frac{s}{\omega_d} + 1 \right) \left(\frac{s}{\omega_t} + 1 \right)}_{Lead}, \quad (6)$$

in which $\gamma = A_\rho$ determines the value of the reset state after the reset action and $(K_p, \omega_i, \omega_r, \omega_t, \omega_d, \omega_f, \gamma)$ is the tuning parameter set. It has been shown that the sequence of controller filters has effects on the performance of reset control systems [23]. In this research, the sequence of control filters is the traditional approach in which the tracking error is the input of the reset element and other linear parts following in series. In this tuning method, the controller is tuned given the following specifications: cross-over frequency ω_c , phase margin ϕ_m , and modulus margin M_m . Note that these specifications are based on the DF analysis or defined pseudo-sensitivities. Furthermore, since the scope of this paper is tuning of the CgLP part, ω_i and ω_f are tuned as $\frac{\omega_c}{10}$ and $8\omega_c$, respectively, to have acceptable tracking and noise rejection performances [8], [21], [24]. To assure stability and use of pseudo-sensitivities, the H_β condition (Theorem 1) has to be satisfied. In addition, a robustness requirement in the form of iso-damping behaviour [1], [25] requires that the phase behaviour of the system must follow

$$\frac{d(\angle \mathcal{N}_{CgLP}(j\omega)PID(j\omega)G(j\omega))}{d\omega} \Big|_{\omega=\omega_c} = 0. \quad (7)$$

All constraints are summarized as

- Cross-over frequency constraint:

$$|\mathcal{N}_{CgLP}(j\omega_c)PID(j\omega_c)G(j\omega_c)| = 1$$

- Phase margin constraint:

$$\angle \mathcal{N}_{CgLP}(\omega_c) + \angle PID(\omega_c) + \angle G(\omega_c) = \phi_m$$

- Modulus margin constraint: $\max |S_\infty(j\omega)| < M_m$
- Iso-damping Behaviour: Equation (7)
- The H_β condition: Equation (5) and $-1 < \gamma \leq 1$

Eventually, we define a suitable cost function for the tuning of the control structure (6). According to [26], to have an appropriate tracking performance in the interested region of frequencies, the following cost function is obtained as

$$J = \max_{\omega \leq \omega_f} \left| \frac{S_\infty(j\omega)}{\omega} \right|_{dB}, \quad (8)$$

in which ω_l determines the interested region of frequencies over which the reset control system is expected to track references and reject disturbances. There are several methods such as grid search, gradient methods, Genetic Algorithm, etc., for solving this problem. Here, since the performance of the controller is not so sensitive to a small change of the tuning set parameter, we suggest to use a grid search method for completing the tuning procedure. The parameter K_p is determined by the cross-over frequency definition. In addition, it is possible to find vectors l_B and u_B to set

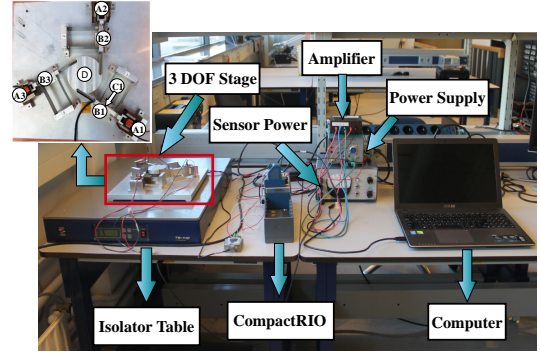


Fig. 2: The whole setup including computer, CompactRio, power supply, sensor power, amplifier, isolator, sensor and, stage

lower and higher limits for $(\omega_r \omega_d \omega_t)$ by the phase margin definition and considering stability of the base linear of the system (i.e. $\omega_c l_B < [\omega_r \omega_d \omega_t]^T < \omega_c u_B$). Then, with a small resolution, we grid the parameters and provide a parameter space. Now, we calculate constraints (3)-(6) for every point in this space, and eliminate the points which do not satisfy the constraints. Finally, suppose there are N tuning parameter sets $(K_p, \omega_r, \omega_t, \omega_d, \gamma)$ which satisfy the aforementioned constraints, then the parameter set which has the minimum J value is selected for designing the control structure (6).

III. PRACTICAL EXAMPLE

To show the effectiveness of the proposed tuning method, a precision positioning stage (Fig 2) is used as a benchmark in this paper. In this stage, which is termed ‘‘Spider’’, three actuators are angularly spaced to actuate 3 masses (indicated by B1, B2, and B3) which are constrained by parallel flexures and connected to the central mass D through leaf flexures. Only one of the actuators (A1) is considered and used for controlling the position of mass B1 attached to the same actuator which results in a SISO system. A linear power amplifier is utilized to drive the Lorentz actuator, and Mercury M2000 linear encoder is used to obtain position feedback with the resolution of 0.1 μm . The identified frequency response data of the system is shown in Fig 3. As shown in Fig. 3, although the plant is a collocated double mass-spring system, the identified frequency response data is well approximated by a mass-spring-damper system with the transfer function

$$G(s) \approx \frac{K e^{-\tau s}}{\frac{s^2}{\omega_f^2} + \frac{2\zeta s}{\omega_r} + 1} = \frac{1.14 e^{-0.00014s}}{\frac{s^2}{7627} + \frac{0.05s}{87.3} + 1}. \quad (9)$$

Note that to use relations provided in [17], the time delay ($e^{-0.00014s}$) is approximated by the first order Pade method [27] as $\frac{-s + 14400}{s + 14400}$. The design requirements for this system are:

- the cross-over frequency: $\omega_c = 100$ Hz
- the phase margin: $\phi_m = 30^\circ$
- the modulus margin: $M_m \leq 6.5$ dB

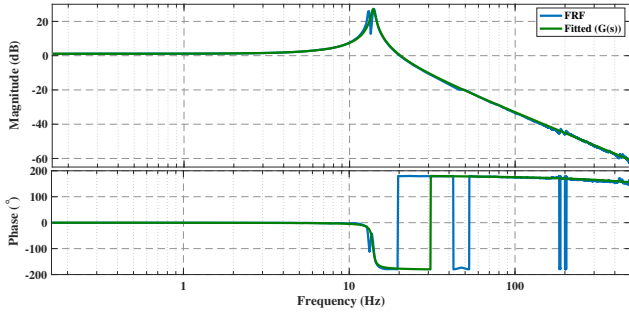


Fig. 3: Identification of the stage

Now, the control structure (6) is tuned based on the described method in Section II-E. To satisfy constraint (7), $\omega_c \leq \omega_l$. Also, in order to not eliminate the low-pass filter effects, $\omega_l \leq \omega_f$. Considering 30° phase margin and stability of the base linear system, it is obtained that $\frac{\omega_c}{5} < \omega_d < \omega_c$. Furthermore, selecting a very small value for ω_r leads to increase the amplitude of high order harmonics at low frequencies which are not desired [15]. Hence, we consider this parameter range $\omega_c [0.05 \ 0.2 \ 1]^T < [\omega_r \ \omega_d \ \omega_l]^T < [1 \ 1 \ 8]^T \omega_c$ in the tuning procedure. In addition, we take $\omega_l = \frac{\omega_c}{10}$ as the maximum limit of the interest region for tracking. The controller is obtained through the proposed tuning method as

$$C_{C_{gLP}} = 25.5 \left(\frac{1}{\frac{s}{111\pi} + 1} \right)^{0.3} \left(\frac{\frac{s}{105.2\pi} + 1}{\frac{s}{1600\pi} + 1} \right) \left(1 + \frac{20\pi}{s} \right) \left(\frac{\frac{s}{105.2\pi} + 1}{\frac{s}{260\pi} + 1} \right). \quad (10)$$

To compare the performance of the tuned controller with a linear controller, a PID structure is also tuned with the same method proposed in Section II-E. To have a fair comparison, the structure of the PID controller is similar to the control structure (6). Finally, the C_{PID} is

$$C_{PID} = 18.46 \left(\frac{1}{\frac{s}{1600\pi} + 1} \right) \left(\frac{\frac{s}{77\pi} + 1}{\frac{s}{520\pi} + 1} \right) \left(1 + \frac{20\pi}{s} \right). \quad (11)$$

Figure 4 shows the open-loop frequency response of the system with controllers C_{PID} and the DF of the open-loop of the system with the controller $C_{C_{gLP}}$. Two systems have the same phase margin and are robust against the gain variation (iso-damping behaviour) as shown in Fig. 4.

The closed-loop frequency responses of the systems with the controller $C_{C_{gLP}}$ including the pseudo-sensitivities and the DF methods, and the closed-loop sensitivities of the system with the controller C_{PID} are shown in Fig. 5. These frequency responses are obtained utilizing the toolbox in [22]. By T_∞ (Fig. 5a), the noise rejection capability of the system with the controller $C_{C_{gLP}}$ must be better than that of the controller C_{PID} . Furthermore, as shown in Fig. 5b, the system with the controller $C_{C_{gLP}}$ has better tracking performance than that one with the controller C_{PID} at frequencies less than 10Hz while the modulus margin of the system with the controller $C_{C_{gLP}}$ is less than that of with the controller C_{PID} . Also, there are discrepancies between the sensitivity DF and

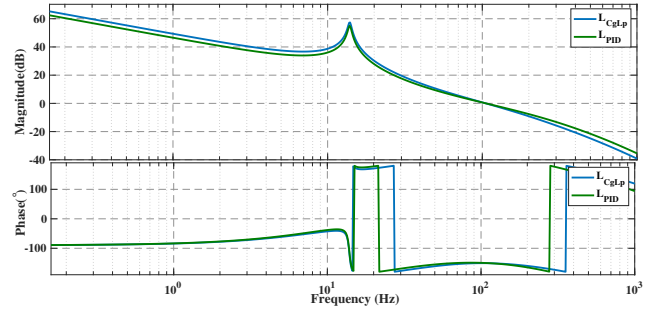


Fig. 4: Open-loop frequency responses of the system with controllers C_{PID} and $C_{C_{gLP}}$

pseudo-sensitivity in the frequency range (30 - 70 Hz) which are due to the existence of high order harmonics.

Based on PS_∞ (Fig 5d), the disturbance rejection capability of the system with the controller $C_{C_{gLP}}$ is better than that of the controller C_{PID} . As shown in Fig.5c, there is a significant difference between the control input of the system with the controller $C_{C_{gLP}}$ and what is predicted by the DF method. In addition, the control input of the system with the controller $C_{C_{gLP}}$ is more than one with the controller C_{PID} . This is explained by the fact that reset elements produce jumps in their output and differentiation of jumps produces a large control input.

A. Time Domain Results

In this part, the time domain results of the designed controllers are compared with each other. To implement controllers (Fig. 6), each controller is discretized with sample time $T_s = 100 \mu s$ using the Tustin method [21], [24], [26]. Furthermore, to provide the well-posedness property [7], [12], there are no reset instants in tandem.

The step responses (step of $10 \mu m$) of the system with these controllers are illustrated in Fig. 7. To assess iso-damping behaviour of the system, the gains of the controllers are varied between 80% to 120% of their nominal values. The step responses have the same rise time while the overshoot of the system with the controller $C_{C_{gLP}}$ are less than that of the controller C_{PID} because the modulus margin of the system with the C_{gLP} compensator is less than one with the PID controller. Furthermore, system with the controller $C_{C_{gLP}}$ has less settling time in comparison with that of with the controller C_{PID} . Besides, step responses of the system with these controllers show iso-damping behaviour indicating. However, $C_{C_{gLP}}$ provides more robustness against gain variation for the system.

In order to compare tracking performances of the systems with both controllers, one triangular reference with the amplitude of $400 \mu m$ (Fig. 8a) and one sinusoidal reference $r(t) = 111 \sin(10\pi t) \mu m$ (Fig. 8c) are applied to the system. As was predicted by S_∞ (Fig. 5b), the system with the controller $C_{C_{gLP}}$ has a better performance at 5Hz (Fig. 8d). In addition, S_∞ (Fig. 5b) precisely predicts the maximum error of the system with the controller $C_{C_{gLP}}$ for the sinusoidal reference. Note that, for the sake of brevity, we only show

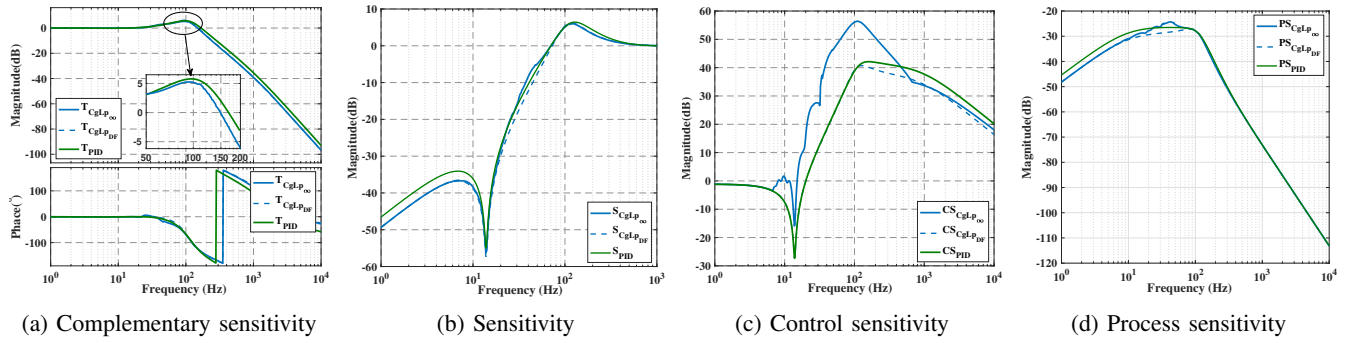


Fig. 5: The DFs (.- DF) and pseudo-sensitivities (.- ∞) of the closed-loop of the system with the controllers C_{CgLP} , and the closed-loop sensitivities of the system with the controller C_{PID}

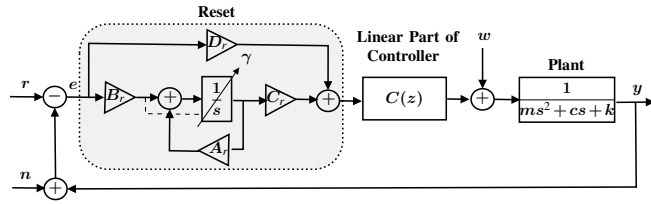


Fig. 6: The block diagram of the whole system for implementing the designed controllers (reset matrices are discretized)

the result at 5Hz while the tracking performance of the system with the controller C_{CgLP} is better than one with the controller C_{PID} for the sinusoidal reference for all frequencies less than 10Hz. As shown in Fig. 8b, the system with the controller C_{CgLP} also has the better tracking performance than that of the controller C_{PID} for the triangular reference (Fig. 8a) which is a combination of several frequencies. For these trajectories, the tracking performance of the system is improved by 30% using the controller C_{CgLP} .

Figure 9 compares the noise and disturbance rejection capabilities of the system with the designed controllers. To study the noise rejection capabilities of the system with the controllers, a white noise with a maximum amplitude of 5 μm is applied to the system. As was expected from T_∞ (Fig. 5a), the noise rejection capability of the system with the controller C_{CgLP} is better than one with the controller C_{PID} (Fig. 9b). It can be said that using C_{CgLP} enhance the noise rejection capability of the system by 40%. In order to evaluate the abilities of the system with the designed controllers for attenuating disturbances, a sinusoidal disturbance $w(t) = 190 \sin(14\pi t) \mu A$ is applied to the system. Similar to the PS_∞ prediction (Fig. 5d), the system with the controller C_{CgLP} has the optimal disturbance rejection performance (Fig. 9a). The disturbance rejection capability of the system is improved by 30% using the controller C_{CgLP} .

To wrap up, the system with the tuned CgLP compensator has less overshoot, the same rise time, better tracking performance for frequencies less than 10 Hz, less modulus margin, better noise and disturbance rejection capabilities than those of the system with the controller PID.

IV. CONCLUSION

This paper has proposed a frequency-domain tuning method for CgLP compensators based on the defined pseudo-sensitivities for reset control systems. In this method, a PID+CgLP structure is considered, and its parameters are tuned such that the pseudo-sensitivity is minimized under several constraints. Also, the tuned CgLP compensator with this method, makes the system robust against gain variations. To show the effectiveness of the proposed approach, the performance of this tuned CgLP is compared with a linear PID. The results show that the frequency framework is reliable for tuning CgLP compensators. Furthermore, the tuned CgLP can achieve more favourable dynamic performance than the PID controller for the precision motion stage. The tracking performance, the disturbance rejection capability, and the noise rejection capability of the system are improved by 30% using the CgLP compensator. Indeed, this method, which allows for tuning in the frequency-domain, opens doors for the implementation of reset controllers in industrial applications.

REFERENCES

- [1] A. A. Dastjerdi, B. M. Vinagre, Y. Chen, and S. H. HosseinNia, "Linear fractional order controllers; a survey in the frequency domain," *Annual Reviews in Control*, 2019.
- [2] I. Horowitz and P. Rosenbaum, "Non-linear design for cost of feedback reduction in systems with large parameter uncertainty," *International Journal of Control*, vol. 21, no. 6, pp. 977–1001, 1975.
- [3] Y. Guo, Y. Wang, and L. Xie, "Frequency-domain properties of reset systems with application in hard-disk-drive systems," *IEEE Transactions on Control Systems Technology*, vol. 17, no. 6, pp. 1446–1453, 2009.
- [4] J. C. Clegg, "A nonlinear integrator for servomechanisms," *Transactions of the American Institute of Electrical Engineers, Part II: Applications and Industry*, vol. 77, no. 1, pp. 41–42, 1958.
- [5] O. Beker, C. Hollot, Y. Chait, and H. Han, "Fundamental properties of reset control systems," *Automatica*, vol. 40, no. 6, pp. 905 – 915, 2004.
- [6] L. Hazeleger, M. Heertjes, and H. Nijmeijer, "Second-order reset elements for stage control design," in *American Control Conference (ACC)*, 2016, pp. 2643–2648.
- [7] Y. Guo, L. Xie, and Y. Wang, *Analysis and Design of Reset Control Systems*. Institution of Engineering and Technology, 2015.
- [8] N. Saikumar, R. K. Sinha, and S. H. HosseinNia, "'Constant in gain Lead in phase' element-application in precision motion control," *IEEE/ASME Transactions on Mechatronics*, vol. 24, no. 3, pp. 1176–1185, 2019.

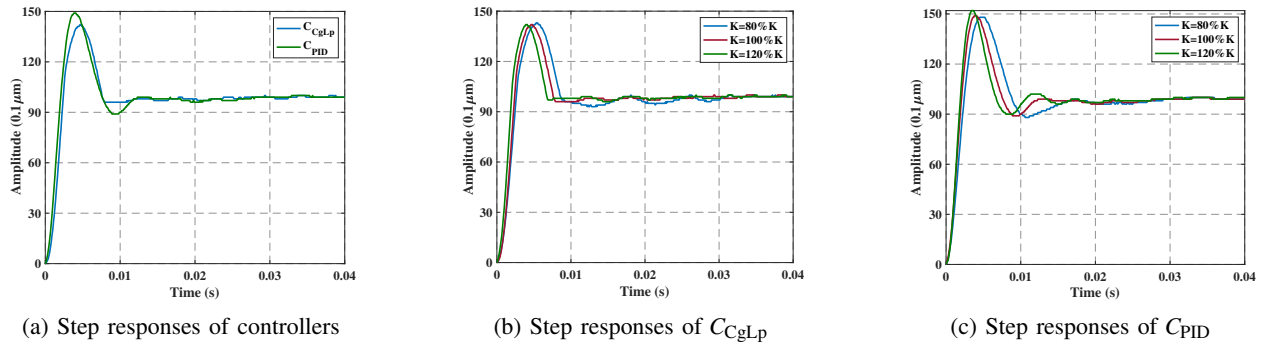


Fig. 7: The step responses of controllers with gain variation between 80% to 120% of their nominal values

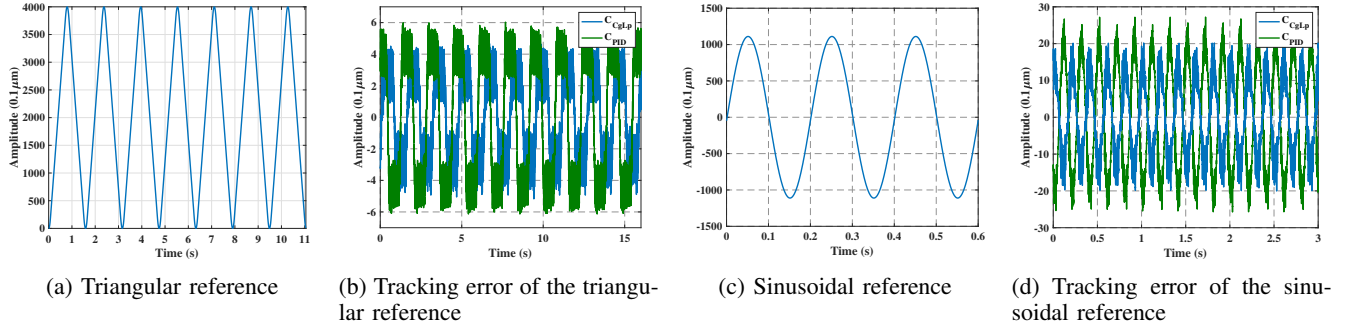


Fig. 8: Tracking performance of the designed controllers for a triangular and a sinusoidal references

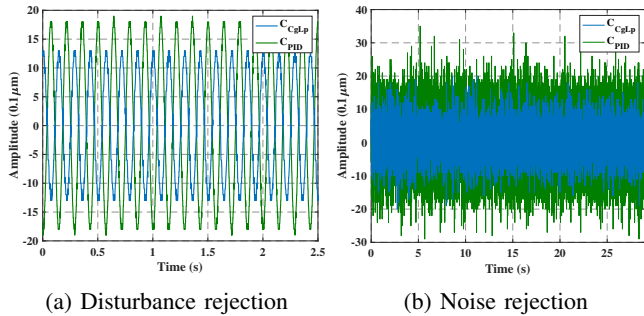


Fig. 9: Disturbance and noise rejection capabilities of the system with the designed controllers

[9] A. Barreiro, A. Baños, S. Dormido, and J. A. González-Prieto, "Reset control systems with reset band: Well-posedness, limit cycles and stability analysis," *Systems & Control Letters*, vol. 63, pp. 1–11, 2014.

[10] A. Baños and M. A. Davó, "Tuning of reset proportional integral compensators with a variable reset ratio and reset band," *IET Control Theory & Applications*, vol. 8, no. 17, pp. 1949–1962, 2014.

[11] J. Zheng, Y. Guo, M. Fu, Y. Wang, and L. Xie, "Improved reset control design for a pzt positioning stage," *IEEE International Conference on Control Applications*. IEEE, 2007, pp. 1272–1277.

[12] A. Baños and A. Barreiro, *Reset control systems*. Springer Science & Business Media, 2011.

[13] S. J. A. M. Van den Eijnden, Y. Knops, and M. F. Heertjes, "A hybrid integrator-gain based low-pass filter for nonlinear motion control," *IEEE Conference on Control Technology and Applications (CCTA)*, 2018, pp. 1108–1113.

[14] D. Valério, N. Saikumar, A. A. Dastjerdi, N. Karbasizadeh, and S. H. HosseinNia, "Reset control approximates complex order transfer functions," *Nonlinear Dynamics*, pp. 1–15, 2019.

[15] H. Xiaojun, A. Ahmadi Dastjerdi, N. Saikumar, and S. HosseinNia, "Tuning of 'Constant in gain Lead in phase (CgLP)' reset controller using Higher-Order Sinusoidal Input Describing Function (HOSIDF)," *Australian and New Zealand Control Conference (ANZCC)*, 2020.

[16] M. Shirdast Bahnamiri, N. Karbasizadeh, A. Ahmadi Dastjerdi, N. Saikumar, and S. HosseinNia, "Tuning of CgLP based reset controllers: Application in precision positioning systems," *IFAC World Congress*, 2020.

[17] A. Ahmadi Dastjerdi, N. Saikumar, D. Valerio, and S. Hassan HosseinNia, "Closed-loop frequency analyses of reset systems," *arXiv e-prints*, p. arXiv:2001.10487, Jan 2020.

[18] A. A. Dastjerdi, A. Astolfi, and S. H. HosseinNia, "A frequency-domain stability method for reset systems," *IEEE 59th Conference on Decision and Control*, 2020.

[19] "Complex order control for improved loop-shaping in precision positioning," in *IEEE 58th Conference on Decision and Control*, 2019, pp. 7956–7962.

[20] S. Polenkova, J. W. Polderman, and R. Langerak, "Stability of reset systems," *Proceedings of the 20th International Symposium on Mathematical Theory of Networks and Systems*, 2012, pp. 9–13.

[21] R. M. Schmidt, G. Schitter, and A. Rankers, *The Design of High Performance Mechatronics High-Tech Functionality by Multidisciplinary System Integration*. IOS Press, 2014.

[22] A. A. Dastjerdi. Toolbox for frequency analysis of reset control systems. [Online]. Available: <https://www.tudelft.nl/en/3me/about/departments/precision-and-microsystems-engineering-pme/research/mechatronic-system-design-msd/msd-research/motion-control/toolbox-frequency-analysis-of-reset-control-systems/>

[23] C. Cai, A. A. Dastjerdi, N. Saikumar, and S. HosseinNia, "The optimal sequence for reset controllers," *18th European Control Conference (ECC)*, 2020.

[24] A. A. Dastjerdi, N. Saikumar, and S. H. HosseinNia, "Tuning guidelines for fractional order PID controllers: Rules of thumb," *Mechatronics*, vol. 56, pp. 26 – 36, 2018.

[25] R. De Keyser, C. I. Muresan, and C. M. Ionescu, "A novel auto-tuning method for fractional order PI/PD controllers," *ISA transactions*, vol. 62, pp. 268–275, 2016.

[26] J. Sabatier, P. Lanusse, P. Melchior, and A. Oustaloup, *Fractional order differentiation and robust control design*. Springer, 2015, vol. 77.

[27] S. Al-Amer and F. Al-Sunni, "Approximation of time-delay systems," *Proceedings of the American Control Conference. ACC (IEEE Cat. No. 00CH36334)*, vol. 4. IEEE, 2000, pp. 2491–2495.